Chinese Chemical Letters 35 (2024) 108385

Contents lists available at ScienceDirect

Chinese Chemical Letters

journal homepage: www.elsevier.com/locate/cclet

Recent advances in long-persistent luminescence materials based on host–guest architecture

Tiantian Wang[a], Man Liu[a], Jiayi Mao[a], Yimeng Liang[a], Lichang Wang[b], Dongzhi Liu[c], Tianyang Wang[a,*], Wenping Hu[a,d,e]

[a] Tianjin Key Laboratory of Molecular Optoelectronic Science (TJ-MOS), Department of Chemistry, School of Science, Tianjin University, Tianjin 300072, China
[b] Department of Chemistry and Biochemistry and the Materials Technology Center, Southern Illinois University, Carbondale, IL 62901, United States
[c] School of Chemical Engineering and Technology, Tianjin University, Tianjin 300072, China
[d] Haihe Laboratory of Sustainable Chemical Transformations, Tianjin 300192, China
[e] Joint School of National University of Singapore and Tianjin University, International Campus of Tianjin University, Binhai New City, Fuzhou 350207, China

ARTICLE INFO

Article history:
Received 20 February 2023
Revised 23 March 2023
Accepted 26 March 2023
Available online 28 March 2023

Keywords:
Organic long-persistent luminescence
Host–guest interaction
Small molecule
Macrocyclic
Polymer

ABSTRACT

Organic long-persistent luminescence (LPL) materials, featuring low preparation cost, eco-friendly synthesis, and easy modification of functional groups, have exhibited extensive applications in information encryption, anti-counterfeiting, and biological imaging. Several design strategies including crystallization-inducement, H-aggregation, and host–guest doping to enhance persistent-room-temperature phosphorescence (RTP) effect by precisely controlling intersystem crossing (ISC) constant and suppressing nonradiative decay rates, those are important strategies to enable LPL performance. Among the strategies, researchers have made several efforts to enhance persistent-RTP effect by host–guest interaction, in which the host matrices provide a rigid environment for phosphor guest molecules. The interaction of the luminescent guest molecules with the host matrix can effectively reduce the vibration and rotation of the luminescent molecules, and suppress the non-radiative inactivation, thereby improving the phosphorescence quantum yield. This review aims to summarize several design strategies of pure organic LPL materials based on persistent-RTP effect through host–guest interaction, and describe some applications of pure organic LPL materials in different fields.

1. Introduction

Organic long-persistent luminescence (LPL) materials have been actively researched and explored in recent years based on persistent room-temperature phosphorescence (RTP) or delayed fluorescence [1–6]. Specifically, organic LPL materials based on RTP effect are extensively applied in the fields of information encryption or anti-counterfeiting, biological imaging, and DNA detection due to some remarkable characteristics such as various emission colors, large Stokes shifts, and long lifetimes [7–16]. However, the triplet excited states of pure organic compounds are easily inactivated by several non-radiative pathways such as oxygen molecules quenching, vibration or high temperature, limiting effectively long LPL phenomenon to nitrogen (or other oxygen-free) environments [17–21]. Several strategies have been studied to achieve persistent-RTP effect *via* precisely controlling intersystem crossing (ISC) constant and suppressing nonradiative decay rates, such as introducing heavy atoms or aromatic carbonyl into the luminescent molecule, crystallization-inducement, polymerization, H-aggregation and host–guest doping [22–32]. In 2017, Adachi *et al.* [1] creatively obtained long afterglow materials lasting for 1 h in N_2 by doping organic phosphors into aromatic host molecules, which provided a guarantee for the rapid development of pure organic LPL materials. Our group has also recently made several efforts *via* host–guest doping to achieve long persistent luminescence.

Host–guest interaction is a kind of the noncovalent interactions in supramolecular chemistry, where the host molecule generally comprises a cavity that specifically recognizes the guest molecule, forming a supramolecular architecture through intermolecular interaction [33–36]. Currently, host molecules are mainly divided into three categories. The first is macromolecules such as cyclodextrin, cucurbituril, calixarene, and crown ether [37–41]. As early as 1995, phosphorescence emission was studied in solution by host–guest interaction of cyclodextrins and halogenated alkanes [42]. Second is small molecules that providing a rigid environment

* Corresponding author.
E-mail address: tianyangwang@tju.edu.cn (T. Wang).

https://doi.org/10.1016/j.cclet.2023.108385
1001-8417/

[43,44]. Lastly, polymers are also a frequently used host molecule [45,46]. Polymer matrices efficiently provide a rigid environment for the guest to achieve ultra-long RTP by host–guest interaction. Furthermore, the use of a polymerous host enables flexibility of LPL crystals fabricated by host–guest interaction.

In the review, we focus on recent advances in pure organic LPL materials based on persistent-RTP effect through host–guest interaction. First, several design strategies of organic LPL materials induced by producing persistent-RTP effect are summarized. Additionally, applications of organic LPL materials are discussed in detail.

2. Mechanism of organic LPL materials based on host–guest architecture

Recently, the mechanism of organic LPL based on host–guest systems including delayed fluorescence and RTP have been extensively explored (Fig. S1 in Supporting information). Up to date, two mechanisms have been confirmed for delayed fluorescence. One is thermally activated delayed fluorescence (E-type delayed fluorescence), and the other is triplet-triplet annihilation (P-type delayed fluorescence) [47].

Generally, most of the reported host–guest RTP systems are fabricated by establishing a rigid environment, which can suppress the nonradiative decay rates of triplet excitons and protect them from being easily quenched. Researchers have found two ways which to create a rigid environment to activate RTP emission. One method is creating a rigid crystalline structure, known as the crystallization-induced phosphorescence effect. The other is doping appropriate guest into rigid host matrix such as polymer directly. Hirata *et al*. [48] first utilized steroid as the host to encase the amino-substituted deuterated carbon and reduce the nonradiative decay, which promoted glaucous persistent RTP with a lifetime longer than 1 s. Compared with a traditional polymeric host matrix [such as polymethylmethacrylate (PMMA)], the steroidal host had lower losses from diffusion. By the approaches mentioned above, the host–guest interactions (such as energy transfer or charge separation) can be well established, aiding in the realization of long-lived RTP emission.

Energy transfers between host and guest molecules play a crucial role in inducing RTP [3,49-54]. Among them, Förster resonance energy transfer (FRET) is considered a feasible explanation why some guest–host materials have RTP properties. The host matrix firstly absorbs the excitation energy, and then FRET between host and guest occurs, eventually leading to phosphorescence emitted by the guest molecules. This strategy needs a large overlap between the emission spectrum of energy donor (host) and the absorption spectrum of fluorescent emitter (guest), and a suitable intermolecular distance between hosts and guests.

Another method of generating RTP phenomenon is through the construction of a donor-acceptor (D-A) system to generate long-lived charge separation. The selected electron donors and acceptors can form a strong charge transfer (CT) state under external excitation, generating free radical anions and cations, and then the generated free radical anions will be separated from the cations by transferring electrons through the acceptor molecules to form a stable charge separated state [1]. When the energy level of the CT state is slightly higher than that of the triplet state of the acceptor, it enables the charge to transfer from the charge separated state to the triplet state of the acceptor, and the energy absorbed by the acceptor can be transferred to the triplet state through the intersystem crossing, realizing the long-life RTP emission. Furthermore, in our recent work we found that this property can be further promoted by utilizing a rigid polymer network. Following these basic design mechanisms and strategies, the long afterglow system will be divided into several parts discussed below.

3. Design strategies of organic LPL materials based on host–guest architecture

Host–guest interaction is a kind of noncovalent interactions in supramolecular chemistry, where the host molecule generally comprises a cavity which specifically recognizes the guest. Currently, host molecules are mainly divided into three categories: small molecules, polymer molecules and macrocyclic molecules. The properties of organic LPL materials based on host–guest architectures were summarized in Table 1.

3.1. Organic LPL materials based on small molecules

Small molecules own the strengths of simple synthesis and easy modification of functional groups, which have received extensive attention by many researchers. The organic LPL materials based on small molecules can achieve efficient and stable RTP emission by constructing a D-A system. It benefits from the rigid environment provided by the host matrix and effectively restricts the molecular vibration, thus suppressing the non-radiative deactivation and reducing the triplet exciton quenching [23,55-57]. In 2011, Kim *et al*. [58] designed a chromophore containing an aromatic aldehyde that generated a triplet state and a bromine that promoted the triplet state. It was doped as a guest molecule into bihalogenated analog host to produce efficient phosphorescence (Fig. 1a). In this article, researchers uniquely combined aromatic carbonyls, heavy atomic effects, and halogen bonds to induce efficient phosphorescence of crystals. In 2017, Adachi *et al*. [1] proposed a long-lived charge-separated state as an intermediate state to realize LPL based on small organic molecules. *N*,*N*,*N*′,*N*′-Tetramethylbenzidine (TMB) with strong electron-donating and 2,8-bis(diphenylphosphoryl) dibenzo[*b*,*d*]thiophene (PPT) with strong electron-receiving were selected as a donor and an acceptor molecule, and lifetime of 2200 ms. Then, the D-A system was constructed by matching energy levels (Fig. 1b). The amorphous film with LPL property was obtained by adopting a melting-quenching method in the nitrogen atmosphere. In the process of photoexcitation, a CT state was formed between TMB and PPT, and then the generated PPT radical anion separated the TMB radical cation from the antiradical anion of PPT by charge hopping diffusion between PPT molecules, forming a stable charge separation state. The gradual recombination of the PPT radical anion and the TMB radical cation gave rise to emission that persisted long after the photoexcitation ceased, resulting in a long afterglow phenomenon. The preparation of this organic LPL material requires high temperature melting and rapid annealing. Moreover, it was required to mix the host and guest materials completely and uniformly. Inspired by the above work, our group has also prepared a series of organic LPL materials by charge separation induced long persistent RTP effect. In addition, considering the convenience and environmental protection of the preparation method, our group [28] prepared doped crystal materials based on two organic small molecules by ultrasonic crystallization. The guest molecule 2,7-di-(*N*,*N*-diphenylamino)-9,9-dimethyl-9*H*-fluorene (DDF) and the host molecule PPT were mixed according to a certain proportion at room temperature. The doped crystal (PPT:DDF) with LPL properties was obtained by means of ultrasonic crystallization in ethanol. It had a high quality single crystal structure with visible LPL properties lasted for more than 6 s under low-energy ultraviolet (UV) excitation, and lifetime of 690 ms (Figs. 1c and d). The signal X-ray analysis showed that the host–guest interaction that led to phosphorescence in PPT:DDF crystals was attributed to the strong intralayer π-π interactions. However, materials mentioned above are prepared and stored under anhydrous and anaerobic conditions, and are easily quenched by water and oxygen in the air, thereby limiting the further application and development. In 2021, our group [43] reported a

Table 1
A summary of properties of organic LPL materials.

No.	Host	Guest	Processing technique	λ_{em} (nm)	τ_P (ms)	Stable in air/water	Ref.
1	PPT	TMB	Melting-quenching	526	2200	No	[1]
2	PPT	DDF	Ultrasonic crystallization	515	690	No	[28]
3	MDPA	DDF2o	Ultrasonic crystallization	523	513	Yes	[43]
4	MDPA	DDF4o	Ultrasonic crystallization	527	319	Yes	[59]
5	MDPA	DDF2n	Ultrasonic crystallization	550	–	Yes	[59]
6	BP	PzPh	Evaporation crystallization	543	3.9	Yes	[4]
7	TPO	PzPh	Evaporation crystallization	547	21	Yes	[4]
8	TP	PzPh	Evaporation crystallization	547	23	Yes	[4]
9	SF	PzPh	Evaporation crystallization	556	836	Yes	[4]
10	TPA	PzPh	Evaporation crystallization	555	428	Yes	[4]
11	DPA	DDFy	Cooling crystallization	525	897.2	Yes	[10]
12	DPA	DDF	Cooling crystallization	530	396.7	Yes	[10]
13	DPA	DDFp	Cooling crystallization	555	75.7	Yes	[10]
14	DPA	2MDDF	Cooling crystallization	510	491.6	Yes	[8]
15	DPA	TPB	Cooling crystallization	515	384.0	Yes	[8]
16	TPP	2MDDF	Cooling crystallization	512	512.6	Yes	[8]
17	TPP	TPB	Cooling crystallization	514	355.6	Yes	[8]
18	2MBP	2MDDF	Cooling crystallization	515	142.6	Yes	[8]
19	2MBP	TPB	Cooling crystallization	518	136.2	Yes	[8]
20	PBPO	TMB	Drop-casting and annealing	526	–	Yes	[69]
21	PVA	DPCz	Drop-casting	488	2044.8	Yes	[70]
22	PEO	BrPCN	Drop-casting	–	–	–	[75]
23	PMMA	BrPCN	Drop-casting	580	6.2	Yes	[75]
24	PVK	BrPCN	Drop-casting	580	0.7	Yes	[75]
25	β-CD-Azo	α-BrNp	Supramolecular self-assembly	528	0.6	Yes	[78]
26	Br-Np-β-CD	AC	Supramolecular self-assembly	512	1.9	Yes	[79]
27	Br-HB-β-CD	AC	Supramolecular self-assembly	500	0.9	Yes	[79]
28	Br-Bp-β-CD	AC	Supramolecular self-assembly	500	2.6	Yes	[79]
29	BrNpA-β-CD	AC	Supramolecular self-assembly	585	1.3	Yes	[79]
30	CB[7]	ANBrNpA	Supramolecular self-assembly	580	0.4	Yes	[84]
31	CB[8]	TBP	Supramolecular self-assembly	565	0.2	Yes	[85]
32	R-NA	TPP	Drop-coating	535	767.3	Yes	[91]
33	S-NA	TPP	Drop-coating	537	788.5	Yes	[91]

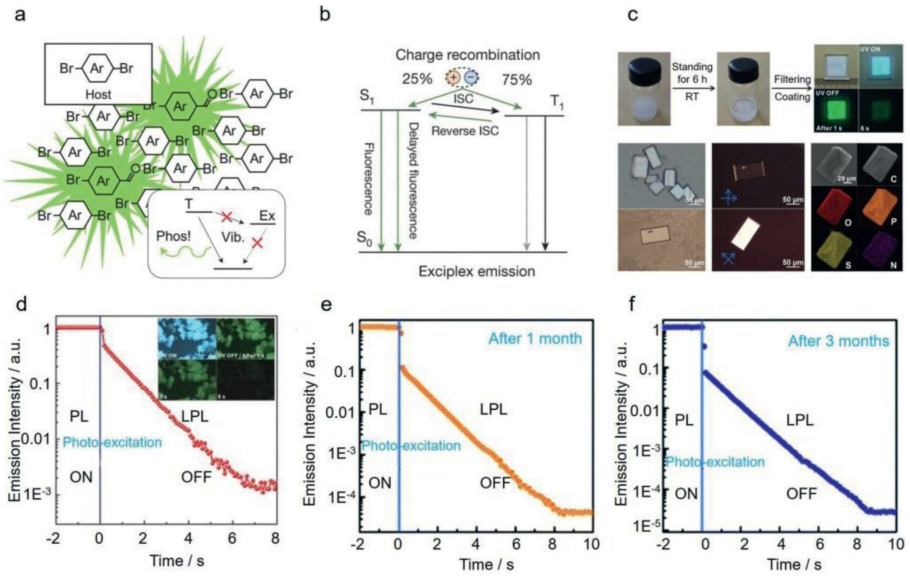

Fig. 1. (a) Schematic diagram of the mechanism and chemical structures of donor-acceptor doped crystals. Copied with permission [58]. Copyright 2011, Springer Nature. (b) Schematic illustration of the mechanism in D-A system. Copied with permission [1]. Copyright 2017, Springer Nature. (c) Preparation process and the morphology picture under microscope of PPT:DDF crystals. (d) Semi-logarithmic plot of the emission decay profile of the PPT:DDF crystal. Panels (c, d) are copied with permission [28]. Copyright 2019, Wiley Publishing Group. (e) Semilogarithmic plot of the emission decay profile of the MDPA:DDF2o crystal from −2 s to 10 s after 1 month. (f) Semilogarithmic plot of the emission decay profile of the MDPA:DDF2o crystal after 3 months. Panels (e, f) are copied with permission [43]. Copyright 2021, Royal Society of Chemistry.

new type of organic doped crystal to overcome this difficulty. We first selected 4-methyldiphenylamine (MDPA) as the host material and DDF derivative 2-*N*,7-*N*-bis(4-methoxyphenyl)-9,9-dimethyl-2-*N*,7-*N*-diphenylfluorene-2,7-diamine (DDF2o) as the guest material. We prepared MDPA:DDF2o crystal with LPL duration time of 8 s by crystallization in aqueous solution, and lifetime of 513 ms. It is so stable under water and oxygen conditions that the LPL properties could be maintained for more than 3 months (Figs. 1e and f). When a trace amount of DDF2o molecules were dispersed and embedded into the crystal structure of MDPA, the charge-separated state DDF2o$^{\bullet+}$-(MDPA)$_n$-MDPA$^{\bullet-}$ could be generated by photo-induced electron or hole transfer, and the generated MDPA$^{\bullet-}$ could undergo electron transfer in the MDPA crystal. And finally achieved the result of high-efficiency separation with the DDF2o$^{\bullet+}$,

thereby realizing a long-lived charge separation state and inducing high-efficiency LPL performance. In this process, LPL efficiency may be affected by the energy level of the charge-separated state formed between the guest and the host. On the basis of this study, we kept the host molecule MDPA unchanged, and promoted the long-lived charge-separated state to transform into the long-lived triplet state of the guest molecule in the D-A system by modifying different functional groups on the guest molecule (Fig. S2 in Supporting information). It effectively regulated the LPL duration time and greatly promoted the development of these types of materials. The guest molecule DDF4o and DDF2n were selected to prepare two other doped crystals MDPA:DDF4o and MDPA:DDF2n with LPL duration time of 6 s and 0 s, respectively [59]. Different generation efficiency of charge-separated state is the main reason for the different LPL duration time. The doped crystal MDPA:DDF2n has no LPL performance because it is not a D-A system and there is no charge-separated state. This indicates that the generation and efficiency of the charge-separated state are two key factors affecting LPL performance, which provides a novel understanding for the design of organic LPL materials.

The reasonable lifetime and color adjustment strategies of organic LPL materials are also extremely important even through few studies have been reported [2,60-63]. In 2021, Huang *et al.* [4] reported a series of host/guest organic phosphorescent materials (UOP) with dynamic lifetime tunable characteristics. 10-Phenylphenothiazine (PzPh) was chosen as the guest material, and a series of organic small molecules with triplet energy levels between the lowest singlet state and triplet state of PzPh were selected as the host materials, namely benzophenone (BP), triphenylphosphine oxide (TPO), tetraphenyl-silane (TPSi), triphenylphosphine (TP or TPP), diphenyl-sulfone (SF) and triphenylamine (TPA) (Fig. 2a). They achieved a wide range of phosphorescent lifetime (from 3.9 ms to 376.9 ms) with invariant afterglow color by doping non-room-temperature phosphors into hosts. The proper three-state energy level of the host matrix provided an effective transition way for the energy transfer between the host and the guest, which was in favor of the generation and stability of three-state excitons. By adjusting the energy gap between the lowest singlet state of PzPh and the lowest triplet state of the host matrix, the ISC and energy transfer processes between them were affected, thus realizing multi-component RTP with a wide range of tunable lifetimes. Xing *et al.* [64] reported a host and guest strategy to achieve color-tunable RTP-based circularly polarized phosphorescence. Bromonaphthalimide with chirality was selected as the guest molecule and tetracyanobenzene was selected as the host to prepare the doped material by simple grinding. When the excitation wavelength was lower than 320 nm, the red RTP and the corresponding circularly polarized luminescence (CPL) was triggered; when the excitation wavelength was higher than 320 nm, the RTP and CPL were turned off, and the blue fluorescence was dominant (Fig. 2b). TCNB provided a rigid environment to stabilize the triplet state of bromine-containing guest molecules, so TCNB molecules had the dual role of triplet sensitizer and stabilizer to synergistically promote the generation of RTP. Recently, our group [10] proposed a two-step strategy to adjust the LPL duration time gradually under ambient conditions. First, three fluorenyl derivatives (DDFy, DDF and DDFp) were selected as guest molecules to be slightly doped into a host molecule diphenylamine (DPA) to obtain the LPL duration and the RTP lifetime which are obviously distinguished in water and air (from 75.7 ms to 897.2 ms) (Fig. 2c). A typical D-A structure could be constructed between the DPA host as an electron acceptor and the DDFx (x = y, p or none) guest as a donor, leading to photoinduced charge separation. The second step was to add the third material deoxyribonucleic acid (DNA), to affect the quenching of RTP, which gradually regulated the LPL duration from the above time limit to 0 s (Fig. 2d).

The preparation method of the doped materials mentioned above is mainly naturally volatilizing and crystallizing in organic solvent, where the crystal size is difficult to control and the repeatability is poor [3,65]. Our group [8] used a simple method to solve the issue of large-scale fabrication and bulk crystallization for doped crystals. Firstly, the guest molecules were fluorene derivatives (2MDDF) and biphenyl derivatives (TPB) [66–68]. For the host molecules, we chose three organic small molecules with a melting point under 100 °C, namely diphenylamine (DPA, 53 °C), TPP (81 °C) and 4,4′-dimethylbenzophenone (2MBP, 95 °C). Guest molecules were doped into a kilogram-scale molten host in water. Then we obtained high-quality doped crystals at room temperature (Fig. 2f). In addition, the trouble of LPL performance being reduced due to lack of bulk crystallization was solved. It was uniformly dispersed with the common high-melting crystal KCl by wet milling in water (Fig. 2e). The LPL of ternary blend crystals had an outstanding reversible temperature response, compared to binary doped crystals, disappearing in the melting state and reducing in the crystalline state.

3.2. Organic LPL materials based on polymer molecules

Although crystal engineering is a common approach to achieve LPL performance, crystal-based LPL materials often have poor flexibility, repeatability, and processability, which obstruct their practical application in the case of requiring flexible, processable and tensile response systems. In order to solve these issues, researchers doped small molecules into polymers which have large molecular weights and functional groups. The interaction between the functional groups can form an oxygen barrier which restricts the molecular vibration to suppress nonradiative decay [22,69-74]. In 2018, Adachi *et al.* [69] reported the first polymer-based pure organic LPL system with TMB as the guest and a poly (aryl ether phosphine oxide) (PBPO) as the host (Fig. 3a). After low-power excitation, the LPL lasted more than 7 min, which was observably longer than the conventional polymer system. It was found that there were incomplete CT and charge separation (CS) states between the small molecule donor TMB and the polymer acceptor PBPO, which caused that the emission duration of the blend was much shorter than that of the small molecule organic long-persistent luminescence (OLPL) system reported in 2017 [1]. Importantly, this polymer-based LPL materials had excellent flexibility and transparency. In 2021, Yang *et al.* [70] also reported organic LPL films with large surface area, good flexibility and high transparency. They doped some organic chromophores into polyvinyl alcohol (PVA) through hydrogen bond and coassembly strategy (Fig. 3b). The flexible films were prepared by drop-casting method. Among them, the DPCz-PVA films exhibit long-lived phosphorescent emission (up to 2044.86 ms) and remarkable LPL duration (more than 20 s). Efficient RTP emission was not only due to the abundant hydrogen-bonding interactions in the PVA matrix, which suppressed the nonradiative decay, but also minimized the energy gap (ΔE_{ST}) between the singlet and triplet states through the coassembly effect. Recently, Ma *et al.* [77] focused on LPL materials with CPL and presented a type of photoinduced circularly polarized phosphorescence materials (CPP) (Fig. 3e). They introduced chiral polymers into the PMMA matrix, and the flexible films with potential CPP emission are fabricated. Amorphous polymers with robust hydrogen-bonded networks provided high RTP quantum yields. UV irradiation for a certain period of time consumed the dissolved oxygen in the PMMA film, and the triplet excitons decayed as phosphorescence rather than being quenched by oxygen molecules, resulting in the photo-induced RTP characteristics. This work will provide an accurate guidance for the design of LPL films with circular polarization characteristic.

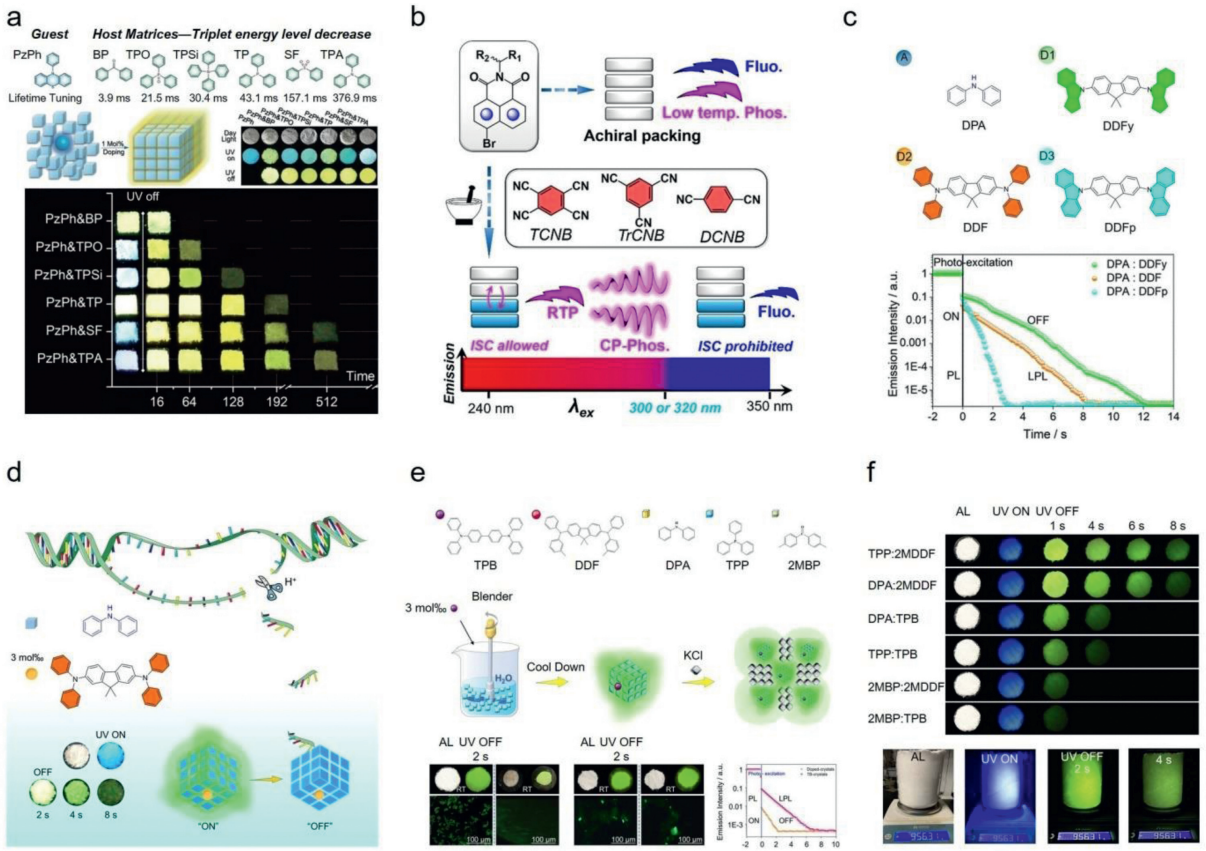

Fig. 2. (a) Chemical structures of PzPh, BP, TPO, TPSi, TP, SF and TPA. Photographs of LPL from the doped crystals. Copied with permission [4]. Copyright 2021, Springer Nature. (b) Design protocol of chiroptical materials by covalent modification and CPP with color-tunable. Copied with permission [64]. Copyright 2021, American Chemical Society. (c) Top: Chemical structures of DPA, DDFy, DDF and DDFp. Bottom: Semilogarithmic plot of the emission decay profile of the doped crystals from −2 s to 14 s. (d) Schematic illustration of the mechanism between doped crystal DPA:DDF and DNA. Panels (c, d) are copied with permission [10]. Copyright 2022, Royal Society of Chemistry. (e) Table of contents of kilogram-scale fabricated organic LPL materials including chemical structures, fabrication process, and LPL properties. (f) The LPL photograph under environmental conditions of the kilogram-scale TPP:TPB doped-crystals. Panels (e, f) are copied with permission [8]. Copyright 2022, Wiley Publishing Group.

It is also important and attractive to achieve stimuli-responsive based on polymers. Yang *et al.* have done some researches in this field. In 2019, Yang *et al.* [75] reported an excitation-dependent long-lived luminescent polymeric system while addressing the issues of processability and color tunability. They doped various pyrene derivatives into PVA and the dopants formed strong hydrogen bonds with PVA, which effectively inhibited the non-radiative deactivation in a rigid amorphous environment. These films showed LPL from blue to yellow and then to deep red under the different wavelength excitation sources (Fig. 3c). The results further confirmed that the luminescence properties of dependent excitation were induced by isolated aggregation states. Based on same mechanism, they reported color-tunable polymeric LPL based on polyphosphazenes in 2020. Two novel polyphosphazene derivatives containing carbazolyl units were doped into PVA films to realize the LPL [76]. The color changed from blue to green with the change of excitation wavelength (Fig. 3d). The dynamic cycle was realized based on the formation and destruction of hydrogen bonds between PVA chains and polyphosphazene derivatives. In theory, each phosphorescent material should have two different phosphorescence in the single-molecular and the aggregate state, respectively, which is expected to achieve a multi-mode response. Aiming to the issue, with the help of the enhancement of spin-orbit coupling by heavy atoms and hetero atoms, Lin *et al.* [65] designed an organic small molecule (BrPCN), which showed RTP in the aggregate and single-molecular states (Fig. 3g). Then they prepared three kinds of films using the drop coating method by doping BrPCN molecules into three polymer matrices, namely, poly(ethylene oxide) (PEO), polymethylmethacrylate (PMMA), and poly(9-vinyl carbazole) (PVK). The dopants were distributed in the polymer matrix in the form of single molecules with three different LPL performances (Fig. 3f). The BrPCN@PVK film showed orange red light while BrPCN@PEO and BrPCN@PMMA films hardly emitted under UV light. After UV radiation, orange phosphorescence of the BrPCN@PMMA film emitted and the quantum yield was up to 13.9% and lifetime of 6.8 ms. The reason was that the oxygen consumption enhanced phosphorescence emission.

3.3. Organic LPL materials based on macrocyclic molecules

The cavity of macrocyclic molecules can restrict the motion of guest molecules and shield them from external quenchers, for which they are widely used to induce and enhance room-temperature phosphorescence. Macrocyclic molecules such as cyclodextrin (CD) and cucurbituril (CB) are commonly used in host–guest doped systems. CD has a large hydrophobic cavity and forms inclusion complexes with guest molecules of appropriate size in aqueous solution. In 1982, Turro *et al.* [81] found that 1-bromonaphthalene and 1-chloronaphthalene could emit obvious phosphorescence in a nitrogen-purified aqueous solution containing β-CD. In 1984, Cline Love *et al.* [82] studied the RTP of non-heavy atom luminophor in cyclodextrin, and first proposed the analysis method of CD-RTP, which became the research hotspot of RTP in aqueous solution. In 2011, Wei *et al.* [83] studied the RTP phenomenon of propranolol (PPL) enantiomers with γ-CD without deoxygenation in the γ-CD supramolecular

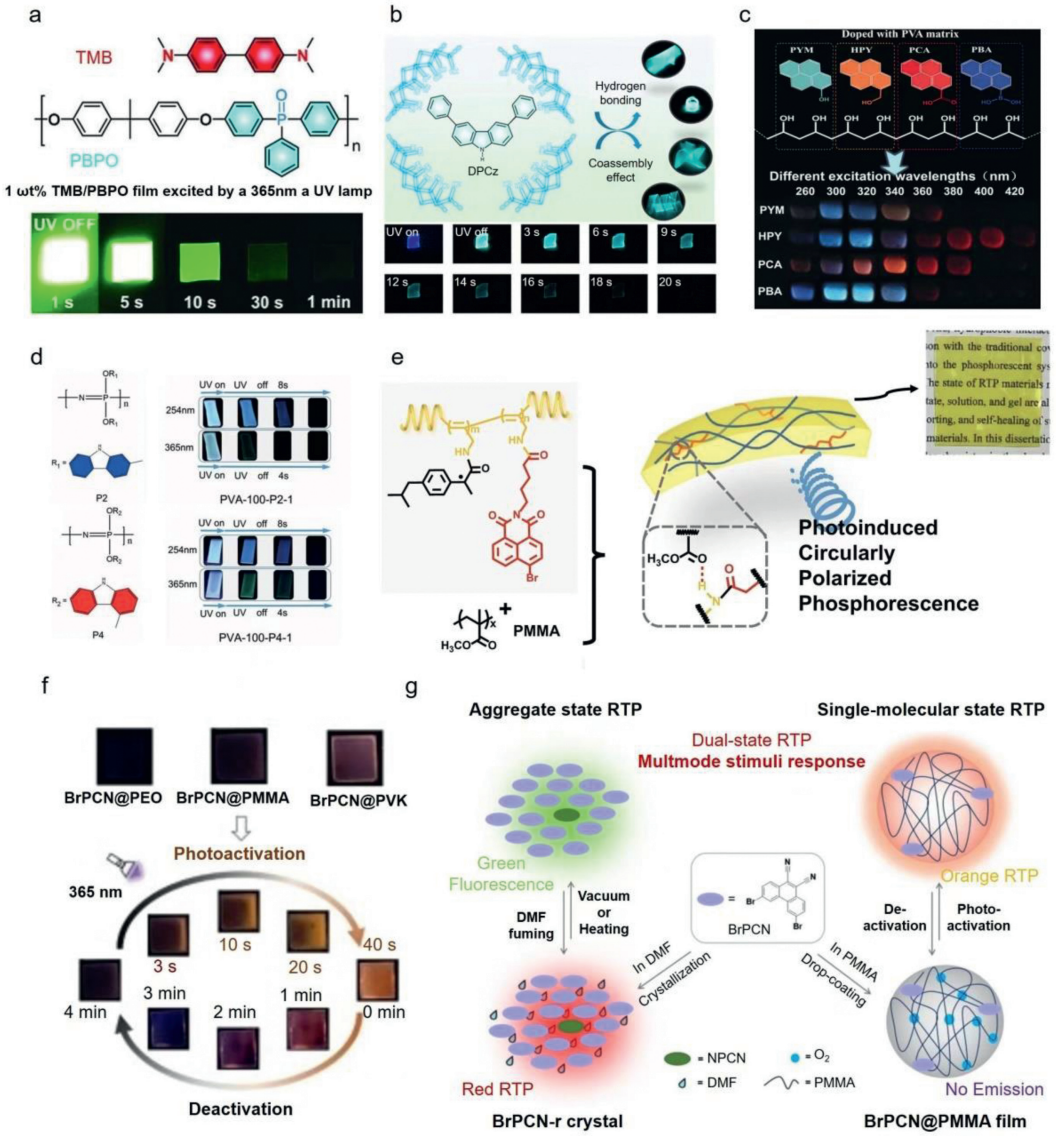

Fig. 3. (a) Chemical structures and LPL photographs of TMB/PBPO film excited by a 365 nm UV lamp. Copied with permission [69]. Copyright 2018, Wiley Publishing Group. (b) Strategy to achieve a long-lived RTP emission by doping DPCz into the PVA matrix. Copied with permission [62]. Copyright 2021, American Chemical Society. (c) Molecular structures of PYM, HPY, PCA, PBA, and PVA, as well as corresponding LPL images of the doped PVA films. Copied with permission [75]. Copyright 2019, Wiley Publishing Group. (d) Chemical structures and LPL images. Copied with permission [76]. Copyright 2020, Wiley Publishing Group. (e) Schematic illustration of the structure and preparation of the p(phNA-*co*-BrNpA)-PMMA film. Copied with permission [77]. Copyright 2022, Springer Nature. (f) Photos of BrPCN@PEO, BrPCN@PMMA and BrPCN@PVK films under UV light. (g) Schematic diagram of RTP multimode stimuli response of BrPCN. Panels (f, g) are copied with permission [65]. Copyright 2022, Elsevier B.V.

system. After adding a small amount of bromocyclohexane, the RTP lifetime of the three-component inclusion complex was significantly different, which was 4.60 ms for *R*-PPL and 5.74 ms for *S*-PPL. Chiral identification of PPL enantiomers could be made by using the difference of afterglow intensity and lifetime. Ma *et al.* [78] constructed a binary system of photocontrolled reversible RTP in aqueous solution based on azobenzene-modified β-cyclodextrin (β-CD-Azo) and α-bromonaphthalene (α-BrNp) (Fig. 4a). In the initial state, β-CD-Azo was in the *trans* configuration in aqueous solution, with the azobenzene embedding into the β-CD cavity. However, the majority of α-BrNp molecules were free in the solution, resulting in a weak RTP emission signal. After 1 h of photoexcitation at 360 nm, the azobenzene unit photoisomerized to a *cis* structure and was removed from β-CD, α-BrNp entered the β-CD cavity. The RTP effect of β-CD-Azo-α-BrNp was obviously enhanced, showing yellow emission with a lifetime of 0.58 ms. In 2018, Wang *et al.* [79] developed a variety of amorphous small molecules by modifying phosphorescent groups onto β-CD. The hydrophobic interaction and intermolecular hydrogen bonding among cyclodextrin derivatives could suppress the phosphor vibration and shield the quencher, which enabled such molecules to achieve efficient RTP emission. The host–guest system was established by pre-assembling BrNp-β-CD with fluorescent guest molecule (1*S*,3*S*)-*N*-(4-((2-oxo-2*H*-chromen-7-yl)oxy)butyl)adamantan-1-aminium chloride (AC) in aqueous solution, and the fluorescence-phosphorescence dual emission and multicolor emission from yellow to purple including white emission were achieved by adjusting the host–guest ratio (Fig. 4b). This research achievement was the first report of amorphous organic small molecule RTP materials, offering a novel strategy for designing amorphous small molecule RTP materials. However, studies mentioned above mainly focus on the regulation

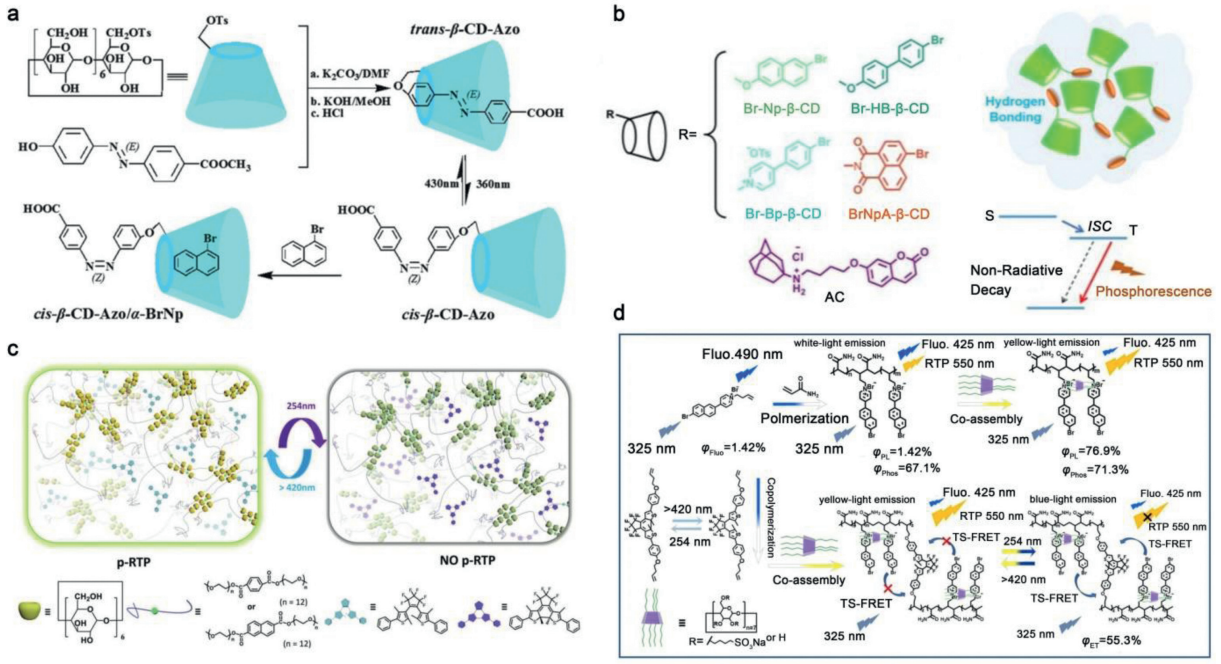

Fig. 4. (a) Synthetic routes of pseudo[1]rotaxane β-CD-Azo. Copied with permission [78]. Copyright 2014, Royal Society of Chemistry. (b) Molecular structures of RTP emissive cyclodextrin derivatives and fluorescent guest molecule AC. Copied with permission [79]. Copyright 2018, American Chemical Society. (c) Photoreversible multicolor p-RTP supramolecular pseudopolyrotaxanes. Copied with permission [80]. Copyright 2022, Wiley Publishing Group. (d) Schematic illustration of the construction of tunable ultrastrong white-light emission. Copied with permission [12]. Copyright 2022, Wiley Publishing Group.

of relatively short lived phosphorescent stimulus response, while there are few studies on long-lived RTP with LPL. Liu *et al.* [80] reported the supramolecular pseudopolyrotaxane system formed by co-assembly of α-CD with benzene and naphthalene modified polyethylene glycol derivatives, respectively, obtaining excited wavelength response and time-dependent multicolor materials (Fig. 4c). The host molecule CDs and the guest molecule formed a pseudopolyrotaxane with a channel-type crystal structure through hydrogen bonding and hydrophobic interaction. The spin-orbit coupling and the formation of ordered structure of pseudopolyrotaxane restricted the nonradiative vibration of phosphors, which was beneficial to the formation of persistent RTP. They also constructed amorphous naphthopyridine-acrylamide copolymers (P-BrNp) with different feed ratios [12]. The monomer BrNp emited a single fluorescence, while the P-BrNp copolymers exhibited an obvious RTP phenomenon. P-BrNp-0.1 had a white-light emission quantum yield of 83.9%, when assembled with sulfobutylether-β-CD (SBE-β-CD), the fluorescence quantum yield increased from 64.1% to 71.3%, and the photoluminescence changed from white to yellow. Reversible RTP emission could be realized through an efficient phosphorescence resonance energy transfer by introducing diarylethene monomers as a photoelectric switch (Fig. 4d). Experiments showed that BrNp was not encapsulated in the cavity of SBE-β-CD, but the electrostatic interaction between BrNp (positive charge) and SBE-β-CD (negative charge) mainly existed in the host–guest system.

Cucurbituril has a cavity surrounded by carbonyl, which forms inclusion complexes with organic guests, and the rigid structure of cucurbituril can better stabilize the triplet exciton of guest molecules [87]. In 2007, Mu *et al.* [88] reported cucurbit[7,8]uril (CB[7] and CB[8]) induced quinoline derivatives to emit RTP in aqueous solution, and found CB[n]-RTP for the first time. The group also studied the RTP phenomenon of α-naphthol and β-naphthol induced by CB[5] in the presence of KI and $TlNO_3$ [89]. Due to the small size of the CB[5] cavity, the vibration of phosphors was mainly limited by the π-π stacking and C-H$\cdots\pi$ interactions between the outer wall of the CB[5] and the aromatic hydrocarbon plane. In 2017, Ma *et al.* [84] established a new RTP system based on CB[7] and bromonaphthalimide derivative ANBrNpA (Fig. 5a). ANBrNpA had no obvious phosphorescence emission, however, after doping with CB[7], the intensity of the phosphorescence spectrum increased significantly, which was attributed to the inclusion effect of CB[7] and BrNpA phosphor. In 2020, supramolecular host–guest assembly strategy was used for the first time to construct a vision-excited pure organic RTP system [85]. RTP emission was achieved in aqueous solution using the host molecule CB[8] and a triazine derivative TBP (Fig. 5b). In addition, multicolor photoluminescence was achieved by dopping different molar ratios of CB[8] to TBP solution. After adding CB[8] into TBP solution, CB[8] directionally contained two TBP molecules under diode-diode interaction, hydrogen bonding and hydrophobic interaction, which further induced the stable CT state with red-shifted excitation wavelength and effectively suppressed the molecular motion.

In 2021, Liu *et al.* [86] reported pure organic supramolecular compound pins composed of alkyl-bridged phenylpyridinium salt and CB[8] with a "one host and one guest" and "head to head" binding formation, which can overcome electrostatic repulsion and promote intracolecular charge transfer (Fig. 5c). The supramolecular pin 1/CB[8] showed the highest phosphorescent quantum yield (99.38%) reported so far after being incorporated into a rigid matrix. Polychromatic photoluminescence including white light can be obtained with different excitation wavelengths and host–guest ratios.

3.4. The introduction of polymer to enhance performance of organic LPL materials based on host–guest architecture

As mentioned above, researchers have made great efforts to obtain purely organic LPL materials by inducing persistent-RTP through host–guest effect. However, triplet excitons are easily

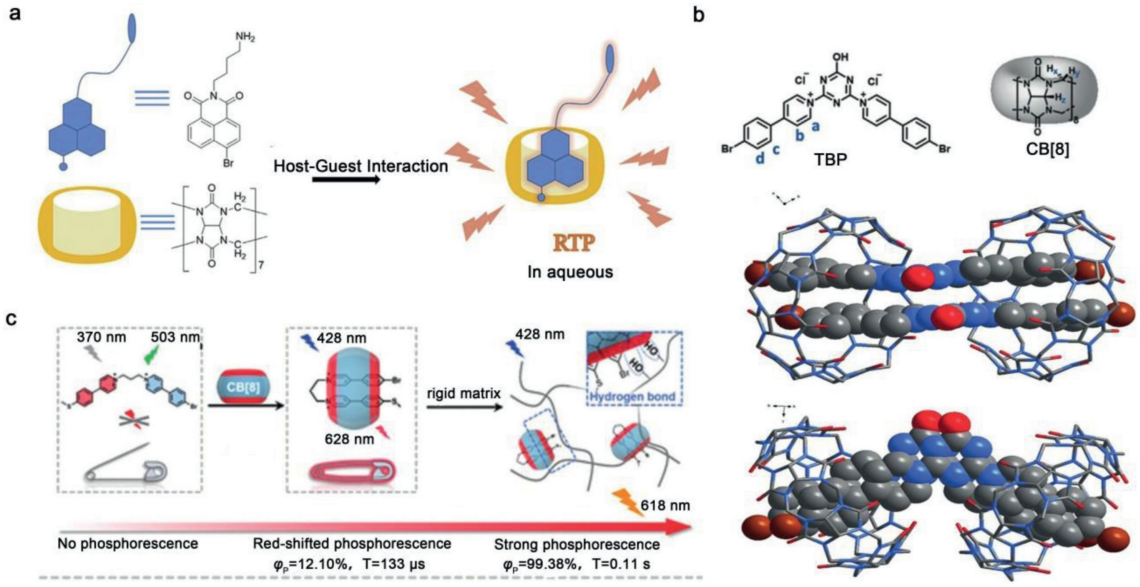

Fig. 5. (a) Schematic representation of the CB[*n*]-RTP system by host–guest interaction between ANBrNpA and CB[7]. Copied with permission [84]. Copyright 2017, Elsevier Ltd. (b) Molecular structures and interaction mode of TBP and CB[8]. Copied with permission [85]. Copyright 2020, Wiley Publishing Group. (c) Views of single-crystal X-ray structure of the $(TBP)_2{\cdot}CB[8]_2$ assembly. Copied with permission [86]. Copyright 2022, Wiley Publishing Group.

quenched by oxygen or other nonradiative deactivation pathways, encouraging us to enhance the performance of pure LPL crystal materials are generally poor in flexibility, repeatability and host–guest doped materials is another widely explored method that will effectively suppress molecular vibration and efficiently obtain LPL emission. The polymer matrix provides a rigid environment for host–guest molecules to effectively improve the luminescence performance of the induced RTP.

Zhao *et al.* [90] proposed to use triphenyl phosphonium bromide polymer (PBNTB, PTNTB) as host, BTBA, TPB and TPBP as guest, doping into the PMMA matrix to achieve flexible luminescent films (Fig. 6a). The results proved that the RTP properties of the materials depended on the grafting ratio of the polymer. With the increase of the grafting ratio, the phosphorescence emission intensity increased sharply (Fig. 6b). In addition, the nonradiative vibrational deactivation of triplet excitons was further reduced with the increase of the grafting ratio of the polymer for obtaining long-lived RTP materials. Our group still has in-depth research in these questions. Wang *et al.* [91] firstly utilized axial chiral molecules (*R*)-1,1′-bi-2-naphthylamine (*R*-NA) and (*S*)-1,1′-bi-2-naphthylamine (*S*-NA) as the guest and TPP as the host consisting of host–guest doping system to induce long-persistent RTP emission by charge separation to achieve LPL performance. Furthermore, LPL duration was successfully improved from 5 s to 10 s with the introduction of rigid polymer matrix such as PMMA and PVP (Figs. 6c and d). The result showed that the crystals prepared by conventional host–guest interaction had weak LPL performance, while the LPL performance of the corresponding vitrified polymer films was markedly enhanced compared with those non-vitrified one. Consequently, the vitrified polymer could effectively improve charge separation efficiency between host–guest, thereby enhancing the RTP performance. The CPL band from 500 nm to 700 nm shown in Figs. 6f revealed that the enantiomers *R*-VP/*S*-VP also kept chiral in the triplet states owing to the inherent axial chirality of the binaphthyl unit of guest. To achieve the flexibility of host–guest crystals, Wang *et al.* [92] firstly prepared two kinds of pure organic host–guest doped crystals with different afterglow times by an aqueous- assisted method. Then flexible polymer films containing the two kinds of doped crystals were prepared by electrospinning, respectively, which still exhibited significant LPL performance (Figs. 6e and g). This work will accelerate development of large-area flexible fabrication of organic LPL materials.

4. Applications of organic LPL materials based on host–guest architecture

As a kind of materials with great potential and function, organic LPL materials have attracted much attention due to its characteristics of good biocompatibility, environmental protection, low synthesis cost and adjustable luminescence. These useful optoelectronic properties allow materials for a large number of progressive applications in biological, chemical, and optoelectronic fields, such as multiplexing information encryption, anti-counterfeiting, bio-imaging, DNA content detection. Some representative applications of pure organic LPL materials based on host–guest doping systems are described below.

LPL materials are commonly employed as information encryption and anti-counterfeiting materials due to unique photometric characteristics of lifetime, color and external-stimuli responsive coding. Recently, our group [8] explored multidimensional information encryption host–guest LPL materials. Taking use of the different melting points of the host, we printed a peach pattern based on DPA:2MDDF crystals covering with QR code based on TPP:2MDDF crystals. When the temperature rose to 60 °C, LPL of peach disappeared, and LPL properties of both patterns disappeared when rising to 85 °C (Fig. 7a). Consequently, the host–guest doping LPL system produced different temperature responses, increasing the security of information encryption. Our group also exploited multidimensional anticounterfeiting systems. Wang *et al.* [91] induced room-temperature circularly polarized phosphorescence (CPP) emission of a pair of chiral guest molecules. Based on the CPP materials, we revealed valid combination of CPL and persistent-RTP that was difficult to replicate in anti-counterfeiting applications. They took use of the difference in CPL signals of the "phoenix" images caused by different guests doping and the significant differences in afterglow time before and after vitrification (Fig. 7b). This work is promising to promote the development of CPP materials and organic RTP systems. However, it is difficult to

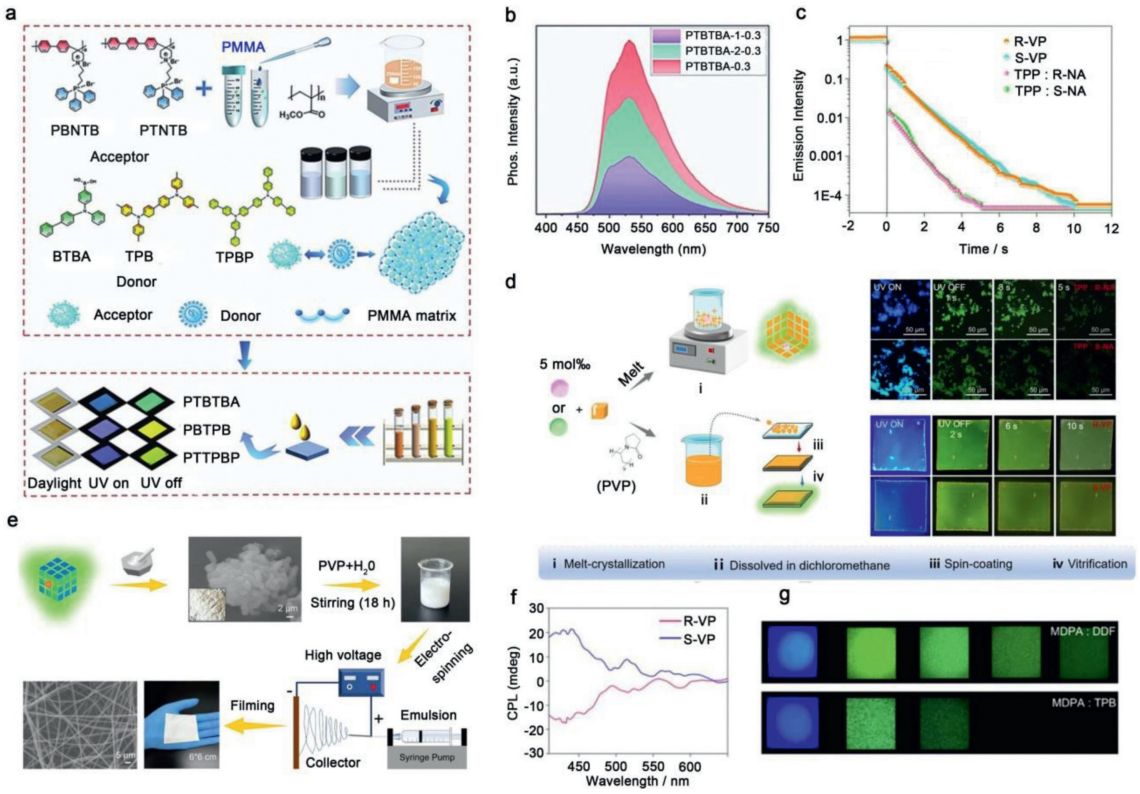

Fig. 6. (a) Schematic diagram for the preparation of long-lived RTP flexible film. Top: Structures of acceptor (PBNTB, PTNTB) and (BTBA, TPB, TPBP). Bottom: Photographs of different flexible films under daylight, UV excitation and after the excitation. (b) Phosphorescence emission spectra of polymer receptor films with different graft rates under 364 nm excitation. Panels (a, b) are copied with permission [90]. Copyright 2022, Wiley Publishing Group. (c) Semi-logarithmic graph of emission decay curves of both doped crystals and vitrified PVP blend polymer films. (d) Preparation diagram of doped crystals and vitrified PVP films, and LPL photographs under 365 nm excitation. (e) Schematic diagram of preparing flexible films containing doped crystals by electrospinning. (f) CPL spectra of the vitrified PVP blend-polymer films *R*-VP and *S*-VP. (g) Photographs of two flexible films under UV light excitation (365 nm) and after excitation. Panels (c, d, f) are copied with permission [91]. Copyright 2022, Wiley Publishing Group. Panels (e, g) are copied with permission [92]. Copyright 2022, Wiley Publishing Group.

identify the CPL signals with the naked eye without a circular polarization spectrometer due to the low dissymmetry *g*-factor (g_{lum}) in most cases. In fact, it is only when $g \geq 1.0$ that applications such as anticounterfeiting become commercially valuable, which means that one of the challenges in the development of CPLPL materials will focus on how to improve CPL characteristics by increasing and regulating the dissymmetry factors (g_{lum}) on a large scale. With the improvement of CPL performance, these kind of pure organic LPL materials will meet the needs of more diversified and special applications. Yang *et al.* [93] constructed an anti-counterfeiting label dependent on ultraviolet illumination by dropping PVA mixture onto a glass substrate (Fig. 7c). Since the efficient RTP emission intensity and lifetime of PVA films are heavily dependent on the degree of cross-linking of PVA, a screen printing technique was successfully fabricated to prepare anti-counterfeiting labels (Fig. 7d).

Long wavelength emissions of long lived phosphorescence are beneficial to reduce tissue scattering and enhancing tissue penetration, thereby organic LPL materials exhibit remarkable superiority in high-resolution imaging. Dai *et al.* [95] reported a class of RTP materials with the ring-fusing effect and host–guest architecture. Nanoparticles (NPs) with good water dispersion and stability were obtained by top-down method using amphiphilic polymer F127 encapsulation materials. The NPs were applied to time-resolved luminescence imaging to eliminate background fluorescence interference. Biological properties of NPs were evaluated by HeLa cells. Under 405 nm laser stimulation, blue and red luminescence appeared in the cytoplasm of the cells, indicating that NPs easily penetrated the cell membrane (Fig. 7f). As shown in Fig. 7g, high-quality long-lived signal was obtained which was easily distinguished from short-lived background fluorescence.

Liu *et al.* [10] developed an analytical method for DNA content detection, which avoided the influence of interferents such as chromophore and fluorophore in vivo and achieved in situ detection which was difficult to achieve with existing methods. To a certain extent, this work expands the conventional application of organic LPL materials.

Another application is organic light-emitting diode (OLED), in which phosphorescent materials with high quantum yield are applied. Host–guest doping systems make chances to achieve higher efficiency for these OLED devices. In 2015, Adachi *et al.* [1] first reported an organic RTP system based on host–guest interaction with lifetime and quantum yield (Q.Y.) of 0.6 s and 4.2%, respectively. In 2019, Wang *et al.* [94] fabricated a host–guest organic RTP systems with Q.Y. of 38% that provided a guidance for achieving high efficiency OLED devices (Fig. 7e). It can be seen that highly efficient phosphorescence systems are desired for better applications of OLED devices. Additionally, organic small molecule optoelectronic materials, such as triphenylamine, indoline and their derivatives, owning advantages of definite molecular structure, relatively simple synthesis and easy purification, have been paid more attention as electron donors in the fields of solid-state solar cells [96–99]. However, the light conversion efficiency of organic solar cells is mostly lower than that of inorganic solar cells due to the defects of organic materials. Therefore, efforts to tune the properties of small molecules to obtain optoelectronic devices fabricated from novel donor-acceptor materials with efficient photoelectric

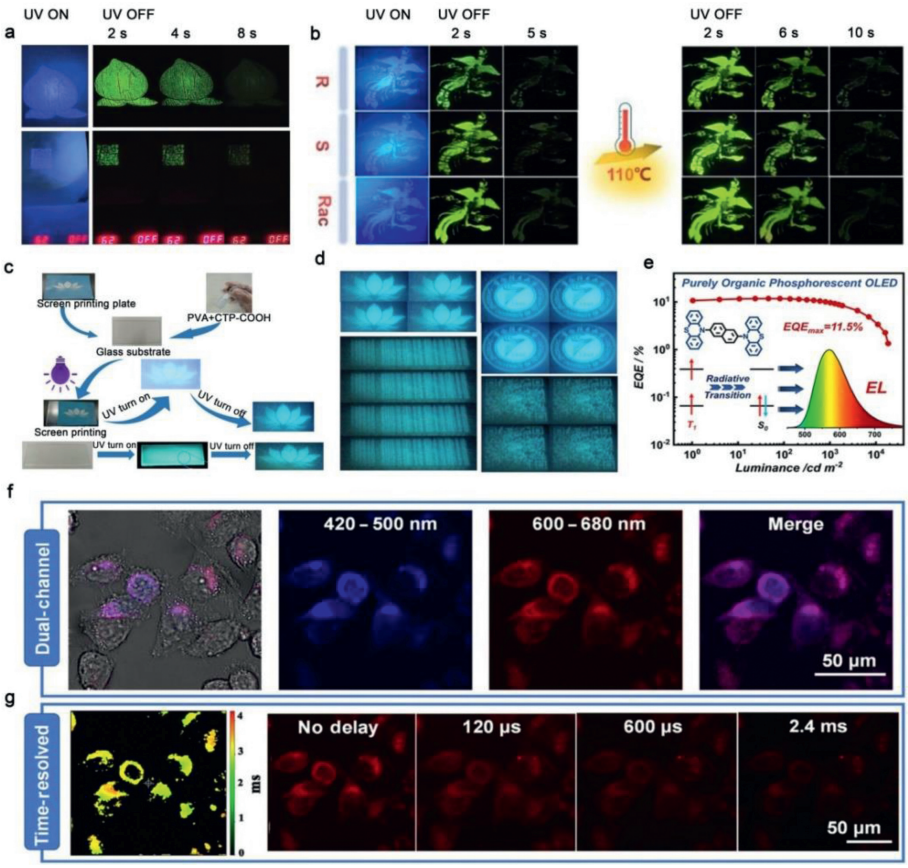

Fig. 7. (a) Photographs of LPL for multi-dimensional information encryption. Copied with permission [8]. Copyright 2022, Wiley Publishing Group. (b) Multidimensional anticounterfeiting application with the effective combination of LPL and CPL performance. Copied with permission [91]. Copyright 2022, Wiley Publishing Group. (c) Screen printing without any inks using the lotus flower screen Plate. (d) Several complex patterns after turning off the excitation. Panels (c, d) are copied with permission [93]. Copyright 2018, American Association for the Advancement of Science. (e) High efficiency OLED was realized using host–guest systems. Copied with permission [94]. Copyright 2019, American Chemical Society. (f) Blue and red luminescence was observed in the cytoplasm of the cells. (g) Left: Intensity of lifetime decay profile of emission band. The rest: Images of HeLa cells at different delay time. Panels (f, g) are copied with permission [95]. Copyright 2021, Chemical Abstracts Service.

conversion have attracted much attention in the field of organic solar cells [100–103].

5. Summary and prospect

The past years have seen remarkable advancement in achieving RTP emission through host–guest interaction, which is an important strategy to enable LPL performance. This review has outlined the recent advances in RTP materials based on host guest structures. Pure organic persistent-RTP can be achieved through host–guest interaction in macrocyclic molecules, organic small molecules, and polymer matrices. Besides, researchers have introduced polymer matrices into host–guest doped materials to enable flexibility and high quantum yield of LPL materials. However, there are still some concerning limitations impeding the achievement of high efficiency RTP emission through pure host–guest interaction. Firstly, the understanding of the mechanism of RTP emission should be further explored while developing new RTP systems, which in turn assists the development of LPL systems. Secondly, one of the common applications of organic RTP materials is biological imaging, while the beneficial emission wavelength is in the near-infrared region. However, there are only a few related studies at present, thereby finding a suitable host matrix is an important way to activate the near-infrared RTP emission. In summary, the rapid advancement of RTP materials through host–guest interaction will provide a convenient strategy for the fabrication of long-time tunable LPL materials in the future.

Declaration of competing interest

The authors declare that they have no known competing financial interests or personal relationships that could have appeared to influence the work reported in this paper.

Acknowledgments

The authors are grateful to National Natural Science Foundation of China (No. 22178263), Natural Science Foundation of Tianjin City (No. 22JCQNJC00770) and Haihe Laboratory of Sustainable Chemical Transformations. The authors also thank Mr. Ben Parks from the Southern Illinois University Carbondale for proofreading the manuscript.

Supplementary materials

Supplementary material associated with this article can be found, in the online version, at doi:10.1016/j.cclet.2023.108385.

References

[1] R. Kabe, C. Adachi, Nature 550 (2017) 384–387.
[2] L. Ma, X. Ma, H. Tian, et al., Angew. Chem. Int. Ed. 61 (2022) e202115748.

[3] B. Chen, W. Huang, G. Zhang, et al., Angew. Chem. Int. Ed. 60 (2021) 16970–16973.
[4] Z. Xie, X. Zhang, W. Huang, et al., Nat. Commun. 12 (2021) 3522–3530.
[5] W. Li, Z. Li, C. Si, et al., Adv. Mater. 32 (2020) e2003911.
[6] Y. Pan, J. Li, K. Zhang, et al., Adv. Funct. Mater. 32 (2022) 2110207.
[7] X. Yao, W. Huang, Z. An, et al., Nat. Commun. 13 (2022) 4890–4898.
[8] M. Liu, J. Zong, T. Wang, et al., Adv. Opt. Mater. 10 (2022) 2201684.
[9] N. Gan, H. Shi, Z. An, W. Huang, Adv. Funct. Mater. 28 (2018) 1802657.
[10] M. Liu, T. Wang, W. Hu, et al., J. Mater. Chem. C 10 (2022) 12249–12256.
[11] J. Ren, Y. Wang, Z. Li, et al., Angew. Chem. Int. Ed. 60 (2021) 12335–12340.
[12] Y.Y. Hu, X.Y. Dai, X. Dong, M. Huo, Y. Liu, Angew. Chem. Int. Ed. 61 (2022) e202213097.
[13] J. Guo, C. Yang, Y. Zhao, Acc. Chem. Res. 55 (2022) 1160–1170.
[14] Q. Xiong, C. Xu, S. Zhang, et al., Chin. Chem. Lett. 30 (2019) 1387–1389.
[15] Y.X. Hu, X. Hao, H.B. Yang, et al., J. Am. Chem. Soc. 142 (2020) 6285–6294.
[16] X. Zhang, J. You, J. Zhang, et al., CCS Chem. 5 (2023) 2140–2151.
[17] Y. Lei, W. Dai, Y. Dong, et al., Mater. Chem. Front. 3 (2019) 284–291.
[18] T. Zhang, X. Ma, H. Tian, et al., Angew. Chem. Int. Ed. 59 (2020) 11206–11216.
[19] G. Qu, Y. Zhang, X. Ma, Chin. Chem. Lett. 30 (2019) 1809–1814.
[20] J. Chen, Y. Chen, Y. Wu, et al., New J. Chem. 41 (2017) 1864–1871.
[21] Q. Xu, L. Ma, X. Lin, Q. Wang, X. Ma, Chin. Chem. Lett. 33 (2022) 2965–2968.
[22] W.L. Zhou, Y. Chen, Y. Liu, et al., Nat. Commun. 11 (2020) 4655.
[23] S. Xu, W. Wang, W. Huang, et al., Nat. Commun. 11 (2020) 4802.
[24] X. Zheng, Y. Huang, Z. Lin, et al., Angew. Chem. Int. Ed. 61 (2022) e202207104.
[25] C. Wang, L. Qu, C. Yang, et al., Adv. Mater. 34 (2022) e2204415.
[26] T. Zhu, T. Yang, Q. Zhang, W. Yuan, Nat. Commun. 13 (2022) 2658.
[27] D. Li, B. Tang, Z. Li, et al., Nat. Commun. 13 (2022) 347.
[28] J. Han, T. Wang, W. Hu, et al., Adv. Funct. Mater. 29 (2019) 1902503.
[29] Z.Y. Xue, J.L. Yu, X.H. Wang, et al., ACS Appl. Mater. Interfaces 14 (2022) 53359–53369.
[30] Z. Wang, T. Li, B. Ding, X. Ma, Chin. Chem. Lett. 31 (2020) 2929–2932.
[31] X. Wang, Z. Chen, J. Yin, S.H. Liu, Chin. Chem. Lett. 33 (2022) 2522–2526.
[32] G. Wang, Z. Wang, B. Ding, X. Ma, Chin. Chem. Lett. 32 (2021) 3039–3042.
[33] M. Xue, Y. Yang, X. Chi, X. Yan, F. Huang, Chem. Rev. 115 (2015) 7398–7501.
[34] P. Li, Y. Chen, Y. Liu, Chin. Chem. Lett. 30 (2019) 1190–1197.
[35] T. Xiao, W. Zhong, L. Wang, et al., Chin. Chem. Lett. 30 (2019) 31–36.
[36] L. Ma, X. Ma, Sci. China Chem. 66 (2022) 304–314.
[37] H. Chen, X. Ma, S. Wu, H. Tian, Angew. Chem. Int. Ed. 53 (2014) 14149–14152.
[38] Z.Y. Zhang, Y. Chen, Y. Liu, Angew. Chem. Int. Ed. 58 (2019) 6028–6032.
[39] W.W. Xu, Y. Chen, Y. Liu, et al., Angew. Chem. Int. Ed. 61 (2022) e202115265.
[40] M. Huo, X.Y. Dai, Y. Liu, Small 18 (2022) e2104514.
[41] P. Wei, X. Zhang, B. Tang, et al., Angew. Chem. Int. Ed. 59 (2020) 9293–9298.
[42] Y. Wei, W. Jin, B. Zhou, et al., Spectrochim. Acta A: Mol. Biomol. 52 (1996) 683–690.
[43] D.Y. Muleta, T. Wang, W. Hu, et al., J. Mater. Chem. C 9 (2021) 5093–5097.
[44] D. Wang, Y. Xie, Y. Dong, et al., J. Phys. Chem. Lett. 12 (2021) 1814–1821.
[45] L. Gao, Y. Zhang, Y. Zhao, et al., Adv. Opt. Mater. 9 (2021) 2101284.
[46] Y. Zhang, Q. Sun, W. Yang, et al., Chem. Eng. J. 447 (2022) 137458.
[47] T. Nakagawa, S.Y. Ku, C. Adachi, Chem. Commun. 48 (2012) 9580–9582.
[48] S. Hirata, K. Totani, C. Adachi, et al., Adv. Funct. Mater. 23 (2013) 3386–3397.
[49] F. Xiao, H. Gao, D. Ding, et al., Nat. Commun. 13 (2022) 186.
[50] Y. Wang, H. Gao, Z. Li, et al., Adv. Mater. 33 (2021) e2007811.
[51] X. Zhen, Y. Tao, K. Pu, et al., Adv. Mater. 29 (2017) 1606665.
[52] J. Yang, X. Wu, Y. Dong, et al., Adv. Funct. Mater. 31 (2021) 2108072.
[53] Y. Liu, Y. Li, F. Li, et al., ACS Mater. Lett. 3 (2021) 713–720.
[54] C.B. Huang, L. Xu, H.B. Yang, et al., J. Am. Chem. Soc. 139 (2017) 9459–9462.
[55] K. Narushima, Y. Kiyota, T. Mori, S. Hirata, M. Vacha, Adv. Mater. 31 (2019) 1807268.
[56] Y. Lei, J. Yang, Y. Dong, et al., Chem. Sci. 12 (2021) 6518–6525.
[57] X. Liu, W. Dai, Y. Dong, et al., J. Mater. Chem. C 9 (2021) 3391–3395.
[58] O. Bolton, K. Lee, J. Kim, et al., Nat. Chem. 3 (2011) 205–210.
[59] J. Song, T. Wang, W. Hu, et al., Dyes Pigm. 193 (2021) 109501.
[60] J. Sun, C. Qian, Z. Ma, S. Wang, Z. Ma, Dyes Pigm. 201 (2022) 110196.
[61] Y. Lei, W. Dai, Y. Dong, et al., Angew. Chem. Int. Ed. 59 (2020) 16054–16060.
[62] H. Liu, D. Ren, L. Ma, et al., Chem. Sci. 13 (2022) 13922–13929.
[63] J. Jovaisaite, S. Kirschner, M. Wagner, et al., Angew. Chem. Int. Ed. 135 (2022) e202215071.
[64] S. An, L. Gao, A. Hao, P. Xing, ACS Nano 15 (2021) 20192–20202.
[65] Y. Huang, X. Zheng, Z. Lin, et al., Chem. Eng. J. 444 (2022) 136629–136638.
[66] X. Chen, W. Dai, Y. Dong, et al., Chem. Eng. J. 426 (2021) 131607–131614.
[67] Y. Ning, J. Yang, B. Tang, et al., Sci. China Chem. 64 (2021) 739–744.
[68] W. Qiu, X. Cai, M. Li, et al., J. Phys. Chem. Lett. 12 (2021) 4600–4608.
[69] Z. Lin, R. Kabe, N. Nishimura, K. Jinnai, C. Adachi, Adv. Mater. 30 (2018) e1803713.
[70] Y. Zhang, Y. Su, Y. Zhao, et al., J. Am. Chem. Soc. 143 (2021) 13675–13685.
[71] Y. Ren, W. Dai, Y. Dong, et al., J. Am. Chem. Soc. 144 (2021) 1361–1369.
[72] H. Wu, D. Wang, B. Tang, et al., Adv. Funct. Mater. 31 (2021) 2101656.
[73] W. Huang, C. Fu, Z. Liang, K. Zhou, Z. He, Angew. Chem. Int. Ed. 61 (2022) e202202977.
[74] L. Ma, S. Sun, B. Ding, X. Ma, H. Tian, Adv. Funct. Mater. 31 (2021) 2101656.
[75] Y. Su, Y. Zhang, Y. Zhao, et al., Angew. Chem. Int. Ed. 59 (2020) 9967–9971.
[76] Z. Wang, Y. Zhang, Y. Zhao, et al., Adv. Mater. 32 (2020) e1907355.
[77] Z. Huang, Z. He, B. Ding, H. Tian, X. Ma, Nat. Commun. 13 (2022) 7841–7849.
[78] J. Cao, X. Ma, H. Tian, et al., Chem. Commun. 50 (2014) 3224–3226.
[79] D. Li, X. Ma, H. Tian, et al., J. Am. Chem. Soc. 140 (2018) 1916–1932.
[80] Y. Zhang, C. Zhang, Y. Liu, et al., Adv. Opt. Mater. 10 (2022) 2102169–2102177.
[81] N.J. Turro, J.D. Bolt, Y. Kuroda, I.J.P. Tabushi, Photochem. Photobiol. 35 (1982) 69–72.
[82] S. Scypinski, L.J. Cline Love, Anal. Chem. 56 (1984) 322–327.
[83] Y. Wei, Y. Ren, J. Li, S. Shuang, C. Dong, Analyst 136 (2011) 299–303.
[84] L. Xu, L. Zou, H. Chen, X. Ma, Dyes Pigm. 142 (2017) 300–305.
[85] J. Wang, Z. Huang, X. Ma, H. Tian, Angew. Chem. Int. Ed. 59 (2020) 9928–9933.
[86] X.K. Ma, W. Zhang, Y. Liu, et al., Adv. Mater. 33 (2021) e2007476.
[87] C. Li, X. Li, Q. Wang, Chin. Chem. Lett. 33 (2022) 877–880.
[88] L. Mu, X.B. Yang, X. Zeng, et al., Anal. Chim. Acta 597 (2007) 90–96.
[89] Z. Gao, X. Feng, X. Gang, et al., Dalton. Trans. 42 (2013) 2608–2615.
[90] C. Wang, Y. Zhang, Y. Zhao, et al., Adv. Funct. Mater. 32 (2022) 211941–211951.
[91] T. Wang, M. Liu, T. Wang, et al., Adv. Opt. Mater. 11 (2023) 2202613.
[92] T. Wang, Y. Song, T. Wang, et al., Dyes Pigm. 207 (2022) 110734.
[93] Y. Su, C. Yang, Y. Zhao, et al., Sci. Adv. 4 (2018) eaas9732.
[94] J. Wang, J. Liang, Y. Wang, et al., J. Phys. Chem. Lett. 10 (2019) 5983–5988.
[95] W. Dai, Y. Zhang, Y. Dong, et al., CCS Chem. 4 (2022) 2550–2559.
[96] T. Wang, X. Zhou, L. Wang, et al., J. Mater. Chem. C 2 (2014) 5466–5470.
[97] H. Sun, L. Wang, X. Zhou, et al., J. Photochem. Photobiol. A 368 (2019) 233–241.
[98] H. Sun, L. Wang, X. Zhou, et al., ACS Appl. Mater. Interfaces 9 (2017) 9880–9891.
[99] H. Sun, L. Wang, X. Zhou, et al., Org. Electron. 61 (2018) 35–45.
[100] T. Wang, X. Zhou, L. Wang, et al., Dyes Pigm. 139 (2017) 601–610.
[101] T. Lu, T. Wang, L. Wang, et al., Dyes Pigm. 136 (2017) 404–415.
[102] C. Zhao, L. Wang, X. Zhou, et al., Dyes Pigm. 137 (2017) 256–264.
[103] T. Wang, L. Wang, W. Li, et al., J. Mol. Struct. 1116 (2016) 256–263.